



Original Paper

Overpressure origins and evolution in deep-buried strata: A case study of the Jurassic Formation, central Junggar Basin, western China



Qiao-Chu Wang^{a, b}, Dong-Xia Chen^{a, b, *}, Xian-Zhi Gao^{a, b}, Mei-Jun Li^{a, b}, Xue-Bin Shi^{a, b}, Fu-Wei Wang^{a, b}, Si-Yuan Chang^{a, b}, Dong-Sheng Yao^{a, b}, Sha Li^{a, b}, Shu-Min Chen^{a, b}

^a State Key Laboratory of Petroleum Resources and Prospecting, China University of Petroleum (Beijing), Beijing, 102249, China

^b College of Geosciences, China University of Petroleum (Beijing), Beijing, 102249, China

ARTICLE INFO

Article history:

Received 5 April 2022

Received in revised form

13 November 2022

Accepted 29 December 2022

Available online 31 December 2022

Edited by Jie Hao and Teng Zhu

Keywords:

Origin of overpressure
Hydrocarbon generation
Tectonic compression
Overpressure transfer
Junggar Basin

ABSTRACT

Overpressure is significant to the exploration and exploitation of petroleum due to its influence on hydrocarbon accumulation and drilling strategies. The deep-burial hydrocarbon reservoirs of Jurassic strata in the central Junggar Basin are characterized by intensive overpressure, whose origins are complex and still unclear. In this study, Bowers' method and sonic velocity-density crossplot method based on well logging data were used as a combination for overpressure judgements in geophysics. Furthermore, the corresponding geological processes were analysed in quality and quantity to provide a rational comprehension of the overpressure origins and the model of overpressure evolution and hydrocarbon accumulation processes. The results showed that hydrocarbon generation in the Jurassic source rocks led to overpressure in the mudstones, while hydrocarbon generation in Permian source rocks led to overpressure in the sandstone reservoirs in Jurassic strata by vertical pressure transfer. The burial and thermal history indicated that the aquathermal effect of pore fluids by temperature increase in deep strata is also an important origin of overpressure, while disequilibrium compaction may not be the dominant cause for the overpressure in deep-buried strata. Furthermore, the continuous tectonic compression in both the north–south and west-east trends from the Jurassic period to the present may also have enhanced the overpressure in deep strata. Meanwhile, the developed faults formed by intensive tectonic compression led to pressure transfer from source rocks to the Jurassic reservoirs. Overpressured geofluids with hydrocarbons migrated to sandstone reservoirs and aggravated the overpressure in the Jurassic strata. To conclude, the intensive overpressure in the central Junggar Basin is attributed to the combination of multiple mechanisms, including hydrocarbon generation, the aquathermal effect, tectonic compression and pressure transfer. Furthermore, the developed overpressure indicated hydrocarbon migration and accumulation processes and the potential of oil and gas reservoirs in deeply buried strata. We hope this study will provide a systematic research concept for overpressure origin analysis and provide guidance for petroleum exploration and exploitation in deep-buried strata. © 2023 The Authors. Publishing services by Elsevier B.V. on behalf of KeAi Communications Co. Ltd. This is an open access article under the CC BY-NC-ND license (<http://creativecommons.org/licenses/by-nc-nd/4.0/>).

1. Introduction

Overpressure is widely developed in many petroliferous basins. The distribution, origins and evolutionary processes of overpressure strongly affect the processes of hydrocarbon generation, migration and accumulation (Baker, 1972; Law and Dickinson, 1985;

Ungerer et al., 1990; Law and Spencer, 1998). The prediction of pore pressure is also of great significance for avoiding risks during drilling work (Zhao, 2003; Tingay et al., 2013). In recent years, deep-buried reservoirs, whose burial depths are near 4500 m, have shown great potential in China, with giant oil and gas fields discovered (Guo et al., 2019; He et al., 2019). The pore pressure in deep burial is usually higher than that in regular reservoirs and is always characterized by intensive overpressure (Zhang et al., 2005; Guo et al., 2019). Therefore, pressure prediction and origin analysis are important but difficult in deep-buried reservoirs owing to the complex distribution and multiple sources of increasing pressure

* Corresponding author. State Key Laboratory of Petroleum Resources and Prospecting, China University of Petroleum (Beijing), Beijing, 102249, China.

E-mail address: lindachen@cup.edu.cn (D.-X. Chen).

(Fan et al., 2012; Guo et al., 2019; Schofield et al., 2019).

Previous studies have shown multiple origins for generating overpressure in mudstones and sandstone reservoirs by geological and geophysical analysis. Disequilibrium compaction and hydrocarbon generation are considered the dominant source for overpressure in mudstones (Hunt, 1990; Osborne and Swarbrick, 1997; Tingay et al., 2009). Fluid expansion, including hydrocarbon generation and fluid volume expansion during temperature increases, is one of the main causes of overpressure in source rocks (Baker, 1972; Law and Spencer, 1998). In addition, clay diagenesis, tectonic compression and pressure transmission are also demonstrated as important overpressure origins (Berry, 1973; Swarbrick and Osborne, 1998; Lahann and Swarbrick, 2011). Analyses of overpressure sources in sandstone reservoirs are rare compared to overpressure analyses in mudstones. Previous studies showed that the overpressure in the sandstone reservoirs of petroliferous basins was mainly from pressure transfer by charging or migration of overpressured hydrocarbons from the overpressured source rocks (Zhao et al., 2017). Furthermore, tectonic compression can also cause overpressure in sandstone reservoirs (Yang et al., 2008, 2016).

Currently, researchers have employed many methods to reveal the source of overpressure. Geophysical methods based on multiple well logs are convenient for judging the origin of overpressure. Bowers' method (Tingay et al., 2007), sonic velocity-density crossplot (Lahann and Swarbrick, 2011; Tingay et al., 2013), porosity and multilogging combination are widely used methods for overpressure source analysis (Teige et al., 1999; Tingay et al., 2009). In addition, geological process analysis, including burial history, thermal history, hydrocarbon generating processes in source rocks, tectonic evolution, diagenetic history and porosity evolutionary processes, can provide information for overpressure generation and preservation (Tingay et al., 2007; Birchall et al., 2021; Li et al., 2021; Wang et al., 2021). In addition, numerical simulation for these geological processes is also used for quantitatively evaluating the pressure increase for each possible overpressure origin by multiple basin modelling software (Liu et al., 2016; Abdel-Fattah et al., 2017; Hakimi et al., 2019).

The Junggar Basin is one of the most petroliferous basins located in northwestern China. Deeply buried sandstone reservoirs in central Junggar Basin (abbreviated CJB) showed great potential as a resource. These reservoirs are characterized by intensive overpressure with the pressure coefficient (which is defined as the ratio of pore pressure and the hydrostatic pressure at the same depth and abbreviated P_{coe}) ranging from 1.2 to 2.1. Some studies indicated that hydrocarbon generation was the dominant overpressure origin (Guo et al., 2019). Furthermore, tectonic compression and vertical pressure transmission were also listed as the sources of overpressure in the central Junggar Basin (Yang et al., 2008, 2011; He et al., 2009).

Existing studies on sources of overpressure in deep-buried strata lack rationality and reliability. First, the currently stated sources of overpressure are not consistent with such intensive overpressure by the repeat formation test (RFT), which is almost twice the hydrostatic pressure. Second, the pressure source judgement was mainly based on a single method instead of multiple methods and without the consideration of the corresponding geological processes. Third, previous analyses often ignored the disparity between deep-buried and regular reservoirs. The differences in burial, thermal and hydrocarbon generating histories may have significant influences on pore pressure. In this research, we used multiple well log-based geophysical methods to systematically analyse the origins of overpressure in the deep-buried sandstone reservoirs in the central Junggar Basin and examined the corresponding geological processes to verify the source of overpressure determined by geophysical methods. Furthermore, we

also hope to reveal the relationship between hydrocarbon migration and accumulation and the evolutionary processes of overpressure in the central Junggar Basin and provide guidance for other deep-buried reservoirs worldwide.

2. Geological setting

The Junggar Basin is one of the most petroliferous basins in China, with an area of approximately $1.36 \times 10^5 \text{ km}^2$ (Cao et al., 2006; Xiao et al., 2010). The basin is located in north-western China and is surrounded by the northern Zhayier Mountains, Halalate Mountains, Delun Mountains, Qinggelidi Mountains, Kelameili Mountains and southern Yilinheibergen Mountains and Bogda Mountains (Fig. 1a). The whole basin is consistent with five first-level tectonic belts, including two depressions and three uplifts (Cao et al., 2006; Qiu et al., 2008; Hao et al., 2011): the Northern Wulugu Depression, Central Depression, Western Uplift, Lvliang Uplift and Eastern Uplift (Fig. 1b).

The central Junggar Basin (CJB) is one of the main oil and gas accumulation regions with multiple oil and gas fields, including the Moxizhuang, Yongjin and Shunbei oil and gas fields (Fig. 1c). The CJB was divided into three tectonic zones, including the northern belt, southern deep burial belt and part of the Changji Depression. The main source rocks in the CJB consist of dark mudstones in the Permian Fengcheng Formation (P_{1f}), Lower Uerhe Formation (P_{2w}), and Upper Uerhe Formation (P_{3w}) and dark mudstones interbedded with coal steams in the Jurassic Badaowan Formation (J_{1b}), Xishanyao Formation (J_{2x}) and Sangonghe Formation (J_{2s}) (Fig. 2). The Permian source rocks were deposited in lacustrine environments. The source rock in P_{1f} was dominated by type I to type II kerogen and characterized by relatively high total organic content (TOC) ($> 1.5\%$) and high maturity, with vitrinite reflectance (R_o) ranging from 1.3% to 1.5% (Cao et al., 2012). The source rocks in P_{2w} and P_{3w} were dominated by type II to type III kerogen and characterized by lower TOC (0.7%–1.4%) and high maturity ($R_o = 1.3\%$ –1.5%) (Cao et al., 2012). The Jurassic coaly source rocks were dominated by type III kerogen with high TOC (5.7% on average) (Dai et al., 2009). The Jurassic source rocks were characterized by low maturity, with R_o ranging from 0.5% to 1.0% (Dai et al., 2009). The main reservoir is dominated by the deltaic sandstones J_{1b} , J_{2x} and J_{2s} . The main seal is the low-permeability shale and mudstone in the Eocene and Neozoic Formations.

The CJB has experienced four main stages since Jurassic period to the present. Since J_{1b} to J_{2t} periods, the Jurassic strata deposited steady and the thickness of the north part was larger than that of the middle and south part (Fig. 3a). From the end of the J_{2t} period, the paleo uplift of the central part of CJB was formed, and the erosion of Jurassic sediments led to the lacuna of J_2 and J_3 formations. After the erosion process, the paleo uplift disappeared (Fig. 3b). From the Cretaceous to Eocene period, the study area experienced a stable depositing period. The faults activities in these periods were rare (Fig. 3c). From the Neogene period to the present, the CJB was influenced by Himalayan Movement, the tilting effect led to a quickly deep burial of the CJB especially for the south part. The structure of anticline formed by the paleo uplift gradually disappeared. At present, the CJB is characterized by a slope belt (Fig. 3d).

3. Distribution of pore pressure

3.1. Pressure distribution by repeat formation test (RFM)

In this research, the pore pressure in the oil reservoirs in the CJB was measured by RFM. We collected 24 RFM data from the Jurassic Formations. The results showed that overpressure mainly

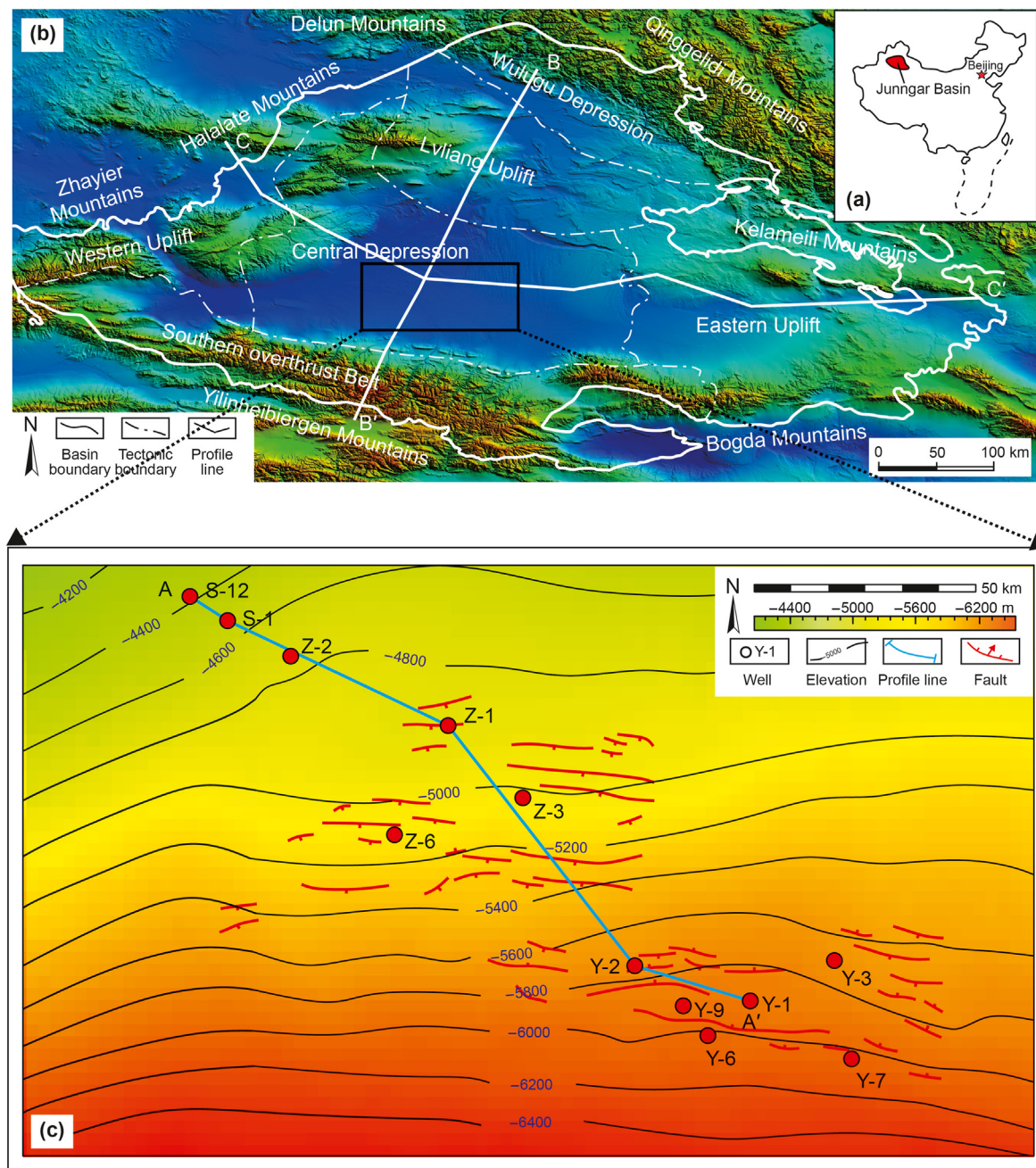


Fig. 1. Location and tectonic belts of the Junggar Basin. (a) The location of the Junggar Basin in China; (b) The tectonic structure and belts of the Junggar Basin and the location of the Central Junggar Basin; (c) The tectonic framework, topographic contour map, well location and development of faults in the Central Junggar Basin.

developed from depths of 4700 m–6200 m (Fig. 4). The pore pressure in the Jurassic reservoirs mainly ranged from 87.8 MPa to 101.5 MPa and even reached 113.5 MPa from depths of 4800 m–6200 m. The P_{coe} in the Jurassic reservoirs mainly ranged from 1.4 to 1.8, with a maximum of 1.93 (Fig. 4). The results indicate that the deeply buried Jurassic Fm. was characterized by intensive overpressure with increasing burial depth.

3.2. Pore pressure profile by Eaton's method

The RFM can only provide some discrete data points of pore pressure in the sandstone reservoirs. Well log-based methods are required to obtain the continuous pressure profile for analysing the

pressure structure and the relationship between sandstone reservoirs and the surrounding mudstones. In this research, Eaton's method (Webster et al., 2011; Wang et al., 2021) was selected as an example to characterize the pore pressure profile for 24 wells. The results of Eaton's method for the Y-1 and Y-2 wells, where the pressure is highest and overpressure is most developed, are shown in Fig. 4.

The pressure structures in the two wells are similar. The sonic well log curve started to deviate the normal compaction trend at the bottom of the Cretaceous Formation (Fig. 5a and c). The residual pressure gradually increased with burial depth, and the P_{coe} in Well Y-1 gradually increased from 1.0 to 1.2 from depths of approximately 4800 m–5700 m in the Cretaceous Formation.

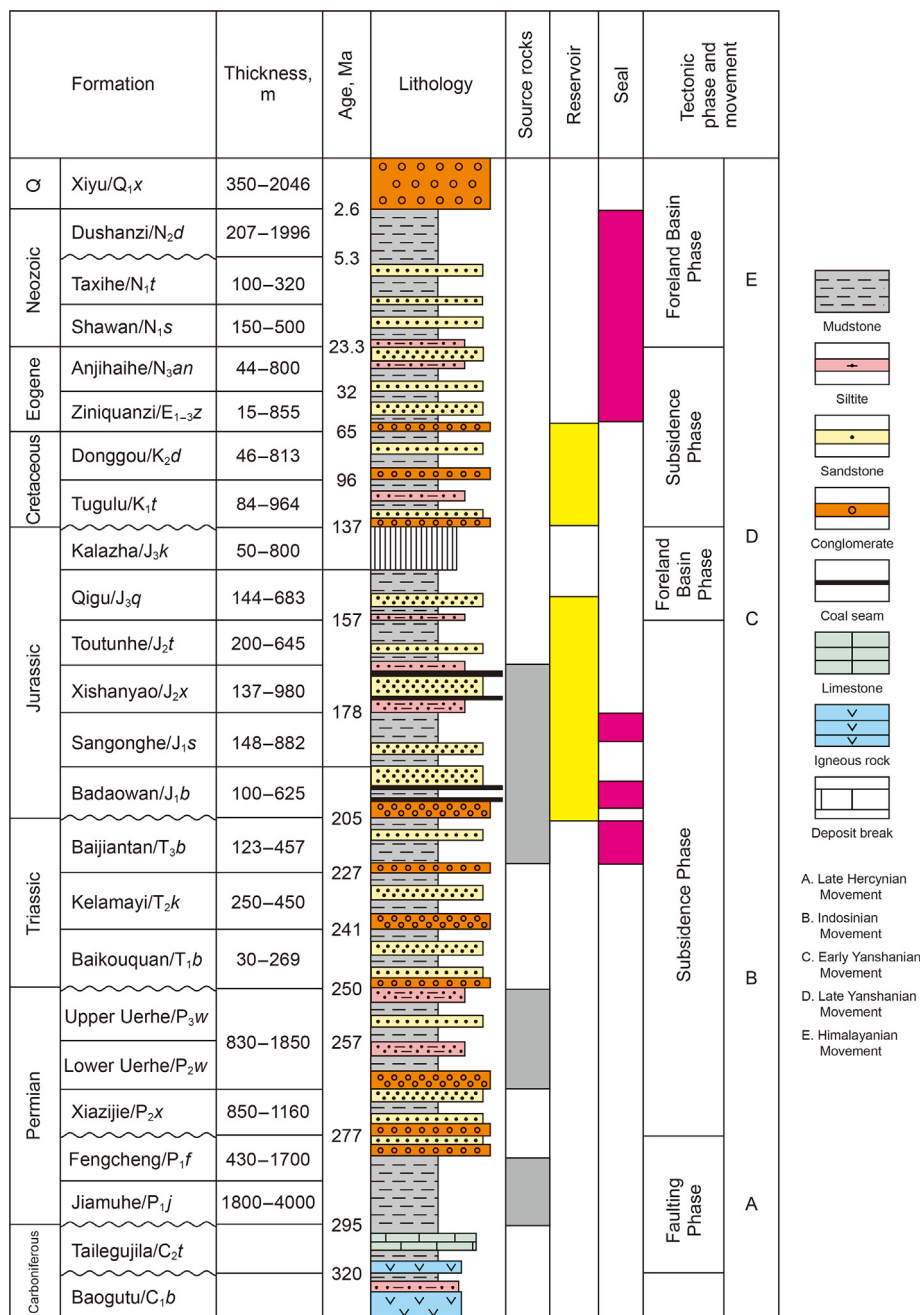


Fig. 2. Generalized stratigraphic column for the central Junggar Basin.

However, the Pcoe in the Jurassic Formation rapidly increased from approximately 1.2 to 1.9 from depths of 5700 m–6300 m (Fig. 5b). The Pcoe in Well Y-2 also showed a gradually increasing tendency in the Cretaceous Formation from depths of 5500 m–5700 m, with the Pcoe increasing from approximately 1.0 to 1.2. The Pcoe in the Jurassic Formation also showed a rapid increasing tendency from depths of 5700 m–6100 m, with the Pcoe increasing from 1.2 to 1.8 (Fig. 5d). The results showed that over approximately 5000 m, the pore pressure was characterized by normal pressure, while residual pressure increased in the Cretaceous Formation, and intensive overpressure was widely developed in the Jurassic Formation. Note that in the Jurassic Formation, the measured pressures by RFM are

higher than those of the surrounding mudstones, which indicates that the deep-buried sandstone reservoirs and the surrounding mudstone may not belong to the same pore pressure system, and the overpressure in the sandstone reservoirs may also not completely originate from the surrounding overpressured mudstones but from the deeper strata.

The cross section A-A' shows the vertical pressure distribution of the CJB from the north to the south portion (Fig. 6). With the deep burial of the strata, the Pcoe in the bottom of the Jurassic Formation (J₁b member) increased from approximately 1.2 to 1.8 from the northern portion to the southern portion. Overpressure also developed in the J₂s and J₂x members in the southern portion of the

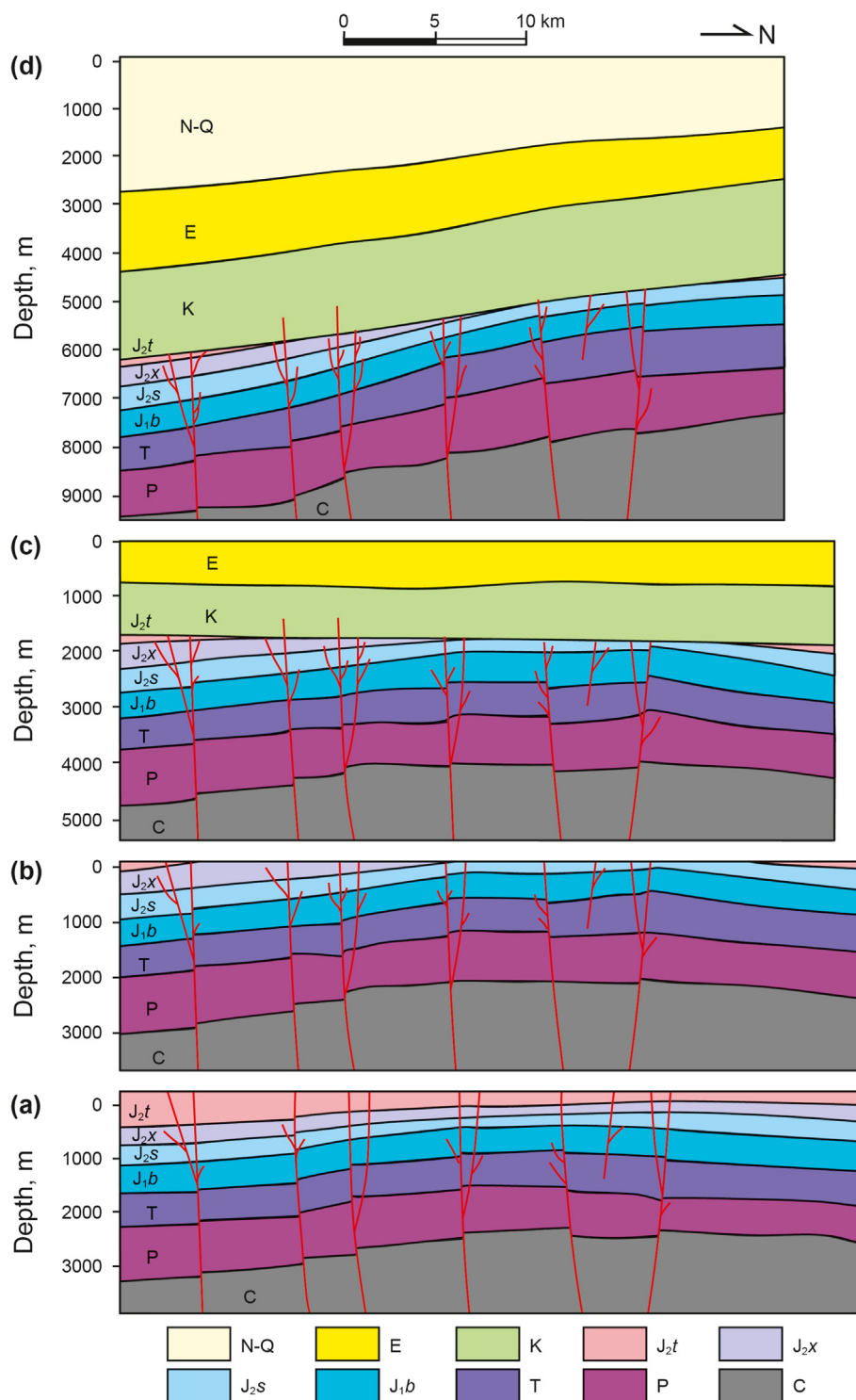


Fig. 3. Tectonic evolution history of the central Junggar Basin. (a) The end of J_{2t} period; (b) The end of Jurassic period; (c) The end of Eogene period; (d) The present.

CJB. However, the J_{2s} and J_{2x} members in the northern portion were characterized by weak overpressure to normal pressure, with P_{co} ranging from approximately 1.0 to 1.2. Note that the overpressure in the sandstone reservoirs in Jurassic strata was usually more intensive than that in the surrounding mudstones with developed faults and petroleum accumulation.

4. Overpressure origins in the CJB

The generation and preservation of overpressure are related to many geological processes. In this section, Bowers' method and sonic velocity-density crossplot method were used as a combination to judge the overpressure origins. Second, the corresponding

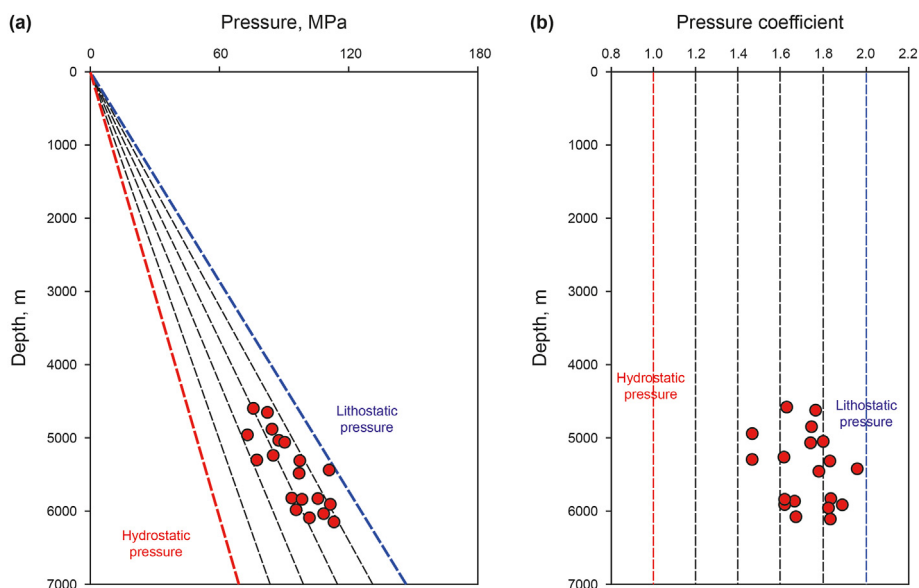


Fig. 4. Distribution of pore pressure (left) and pressure coefficient (right) measured by the repeat formation test.

geological processes were discussed for the possibility and rationality of the overpressure origins.

4.1. Overpressure origins analysis by Bowers' method

Bowers' method was proved as an effective method to analyse the overpressure origins in many petroliferous basins (Bowers, 2002; Tingay et al., 2009, 2013). Bowers' method used vertical effective stress and sonic velocity log or density log data to construct the loading and unloading curve. Bowers claimed that the overpressure caused by disequilibrium compaction and fluid expansion was reflected by the loading curve (the green curve in Fig. 7a and b) and unloading curve (the red curve in Fig. 7a and b). The unloading curves were characterized by two features: (1) sonic velocity showed little change when vertical effective stress increases or decreases (Fig. 6a); (2) sediment density showed little change when vertical stress increases or decreases (Fig. 6b). Previous studies also indicated that the overpressure by clay diagenesis (Lahann and Swarbrick, 2011), pressure transfer (Tingay et al., 2007) and tectonic compression could also be reflected by the unloading curve (Zhao et al., 2017). Therefore, Bowers' method in this research was mainly used to distinguish overpressure by disequilibrium compaction.

The vertical effective stress was calculated by density logs and measured pore pressure by RFM and overburden pressure gradient in the CJB according to Tingay et al. (2007). The result of the Y-1 well showed that the overpressured points fit the unloading feature, which was almost on the unloading curves (Fig. 8a and b). The distribution of overpressured points indicated that disequilibrium compaction might have less of a contribution to the overpressure in the CJB. The utilization of Bowers' method on Well Y-2 also showed a similar feature of overpressured points (Fig. 8c and d). However, the Bowers' method cannot specify the overpressure origins by unloading processes. Therefore, the sonic velocity-density crossplot method and multilogging method were also used.

4.2. Overpressure origins analysis by sonic velocity-density crossplot method

The sonic velocity-density crossplot method has been widely

used for overpressure origin analysis (Tingay et al., 2013; Lahann and Swarbrick, 2011; Liu et al., 2016). In the crossplot of sonic velocity and density, both normal and disequilibrium compaction points fit the loading curve, and the overpressure by unloading fit the unloading curve. However, the crossplot can identify some specific overpressure origins: (1) overpressure caused by fluid expansion is characterized by little change in density with obvious change in sonic velocity (yellow arrow in Fig. 9); (2) overpressure caused by chemical compaction or clay diagenesis is characterized by little change in sonic velocity with obvious change in density (purple arrow in Fig. 9); and (3) overpressure caused by load transfer or combined mechanisms of multiple overpressure origins are characterized by some changes in both sonic velocity and density (green arrow in Fig. 9).

The result in Well Y-1 showed that the overpressured points were characterized by unloading features. Most of the red overpressured points fit the origin of load transfer or combined mechanisms, while some overpressured points indicate that fluid expansion might contribute to the overpressure in the Jurassic stratigraphy (Fig. 10a). This result was consistent with the result of Bowers' method in Well Y-1. The overpressured points in Well Y-2 were mainly characterized by overpressure of load transfer or combined mechanisms (Fig. 10b). The red overpressured points in Jurassic strata indicate that intensive overpressure in Jurassic strata might be attributed to fluid expansion, load transfer or combined mechanisms. To conclude, the crossplot of sonic velocity and density again demonstrated that the overpressure in the deep strata in the CJB had little link to disequilibrium compaction but was indeed caused by multiple origins, which may be attributed to fluid expansion, load transfer, and tectonic compression.

5. Geological responses to overpressure origins

The overpressure origin analysis based on well-logging data provided some clues and evidence for multiple overpressure origins in the CJB. However, the rationality and reliability of the analysis needs further study by examining the geological process for each possible overpressure origin. In this research, the burial history, thermal history, hydrocarbon generating process and tectonic movement were analysed for multiple overpressure origin analysis.

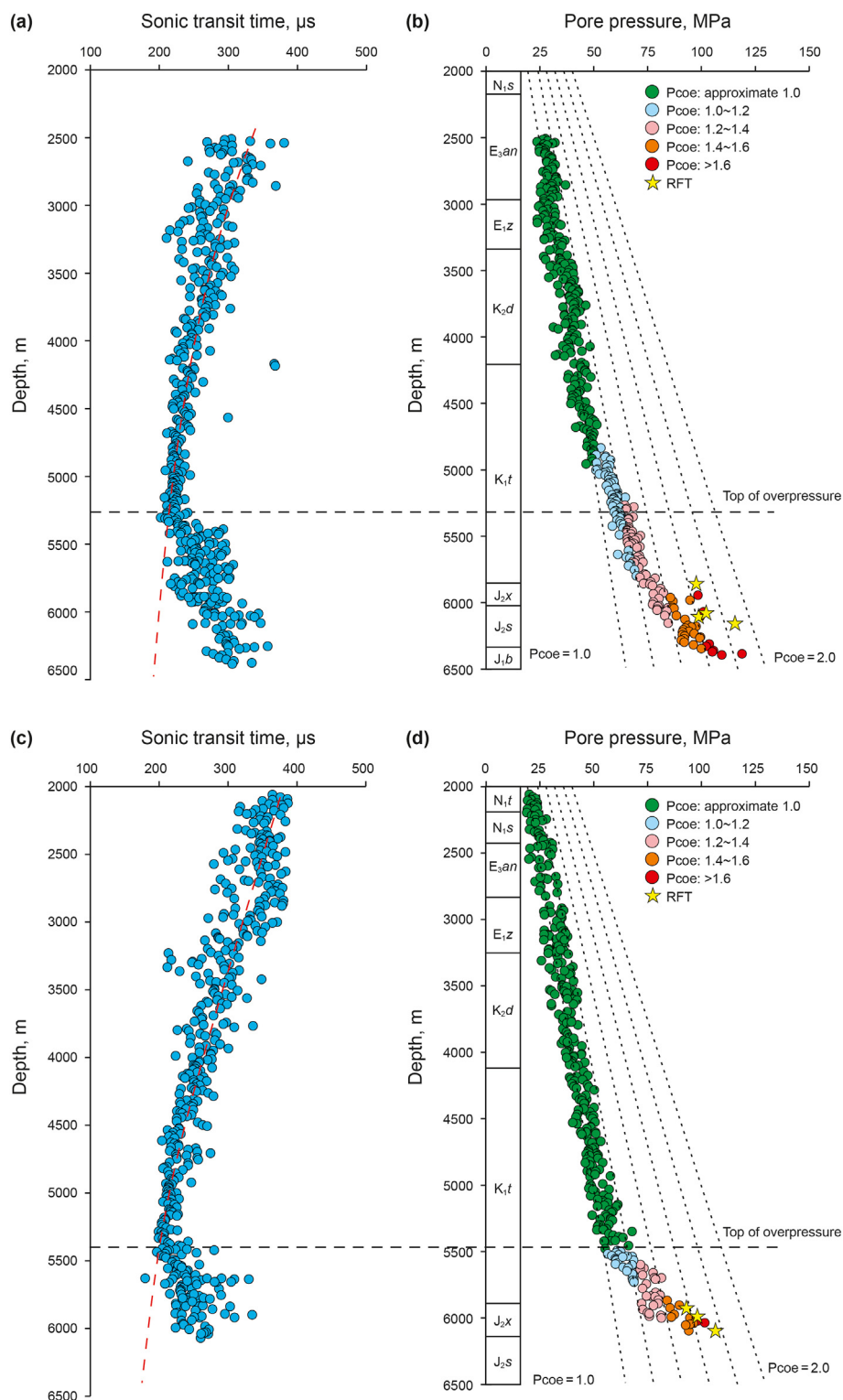


Fig. 5. Pore pressure profile by Eaton's method in Well Y-1 and Well Y-2 in the central portion of the Junggar Basin. Fig. 4(a) and (b) are distribution of sonic transit time and pore pressure of Well Y-1; Fig. 4(c) and (d) are distribution of sonic transit time and pore pressure of Well Y-2.

5.1. Burial history and disequilibrium compaction

Disequilibrium compaction was once considered one of the dominant overpressure origins (Timko and Fertl, 1971; Tingay et al., 2009). In a basin with a high sedimentation rate, the fluids in the low-permeability rocks (usually mudstones) cannot expel fast

enough and are then maintained in the pores of the rocks, leading to an increase in pore pressure. The burial history indicated that the CJB experienced a relatively slow depositional process from the Cretaceous period to the present without obvious rapid burial of sediments (Fig. 11). Previous studies also showed that the sedimentary rate in the CJB was only between 10 and 20 m/Ma, with a

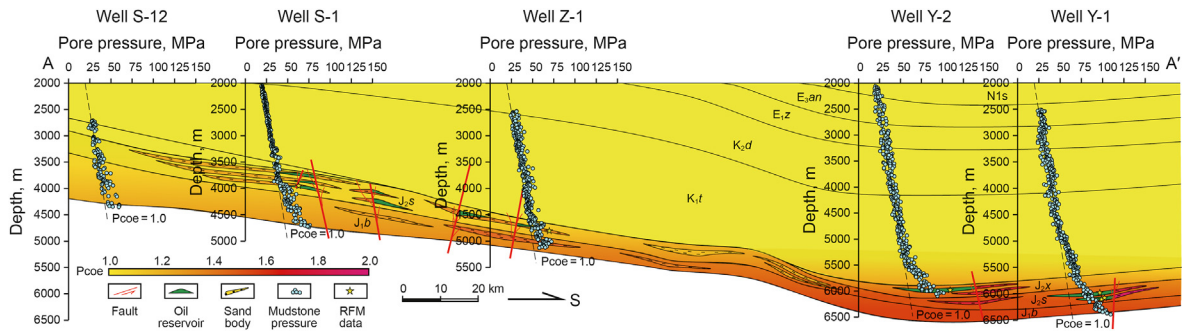


Fig. 6. Pore pressure distribution of the cross section from A-A' in the central Junggar Basin. The location of profile A-A' is shown in Fig. 1.

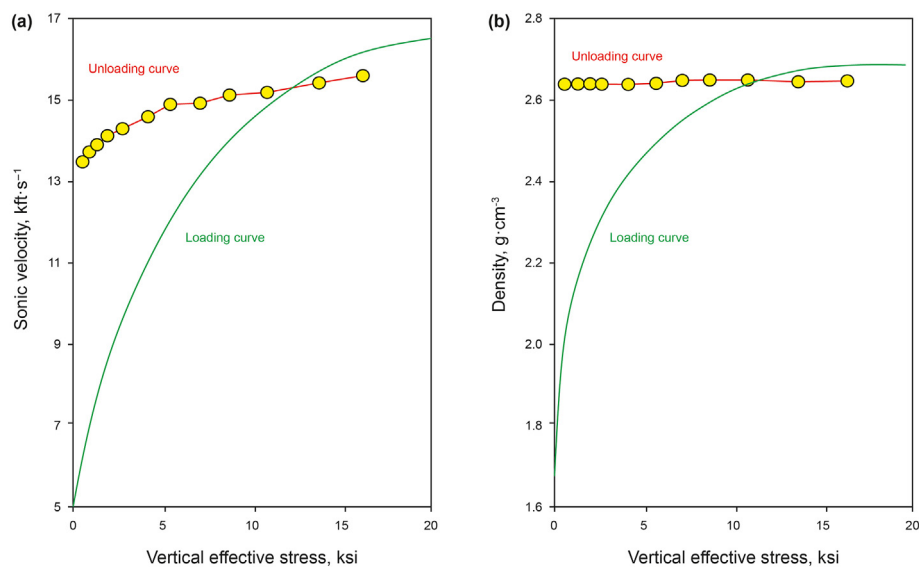


Fig. 7. Plate of Bowers' method (Modified by Bowers, 2002).

maximum rate of approximately 30 m/Ma (He et al., 2018), which is too low to provide the conditions for disequilibrium compaction. Some researchers claimed that only if the sedimentary rate was over approximately 100 m/Ma could disequilibrium compaction occur (Zhang et al., 2005). Furthermore, recent studies have indicated that disequilibrium compaction is mainly generated in strata with burial depths of less than 2000–3000 m (Teige et al., 1999; Zhao et al., 2017). As a deep burial process, the unbalanced state of disequilibrium compaction gradually diminishes with time (Zhao et al., 2017; Li et al., 2021). Therefore, the deep-buried Jurassic sediments in the CJB not only lack the condition of generating disequilibrium compaction but also cannot satisfy the requirement of preservation of overpressure by disequilibrium compaction.

5.2. Thermal history and fluid expansion

According to the results of well log-based methods, fluid expansion was considered one of the main overpressure origins in the CJB. On the one hand, hydrocarbon generation will increase the volume in the pore space of rocks and lead to pressure increase; on the other hand, the higher formation temperature will cause thermal expansion of pore fluids and lead to overpressure.

5.2.1. Hydrocarbon generation

Hydrocarbon generation is an important overpressure origin in petroliferous basins (Law and Dickinson, 1985; Lash and Engelder,

2005; Liu et al., 2021a,b). For the source rocks, the volumes of oil and gas during the hydrocarbon generating processes are much larger than the consumed volume of solid kerogen, which will lead to intensive overpressure in the organic rich mudstone or shale (Timko and Fertl, 1971; Jin and Johnson, 2008; Liu et al., 2021a,b). On the other hand, overpressured fluids with oil and gas will be injected into sandstone reservoirs when the overpressure in the source rocks is large enough to break through the lithostatic pressure and therefore lead to overpressure in reservoirs (Roberts and Nunn, 1995; Caillet et al., 1997).

There are two main source rocks in the CJB: mudstones in the Jurassic Xishanyao Fm, Sangonghe Fm and Badaowan Fm and dark shales in the Permian Wuerhe Fm and Fengcheng Fm. To analyse the overpressure in mudstones in the Jurassic, the 1-D model of the hydrocarbon generating process of Well Y-1 was constructed (Fig. 12). The results showed that the Jurassic source rocks reached the mature stage in the Late Cretaceous (approximately 87 Ma) and generated hydrocarbons (Fig. 12). From the Late Cretaceous to the present, the hydrocarbon-generating process could have caused overpressure in the mudstones, which was reflected in the pressure profile of Well Y-1 (Fig. 4).

It should be noted that the pore pressure in the Jurassic reservoirs (measured by RFM) was higher than that in the Jurassic mudstones, which indicated that the sandstone reservoirs and the surrounding mudstones might not belong to the same pressure unit. In other words, the oil and gas in the Jurassic reservoirs might

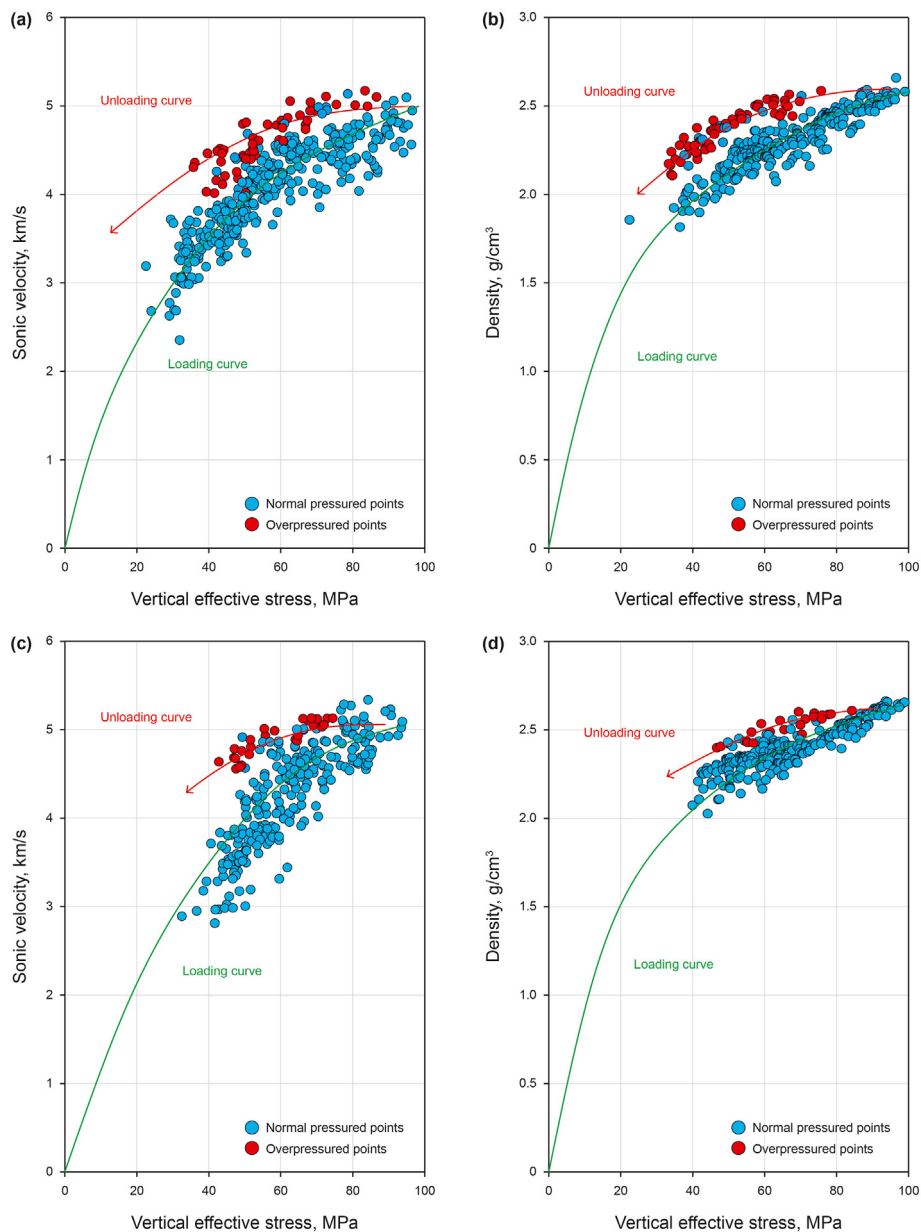


Fig. 8. Overpressure origin analytical results by Bowers' method for (a) (b) Well Y-1 and (c) (d) Well Y-2.

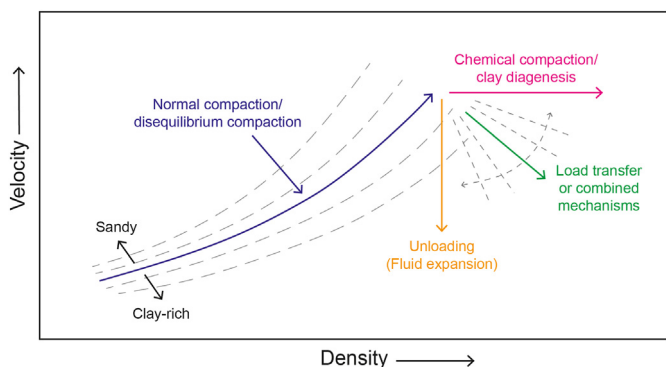


Fig. 9. Plate of the sonic velocity-density method for overpressure origin analysis (adapted from Tingay et al., 2007).

not only have migrated from the Jurassic source rocks but also from the source rocks from other formations. The hydrocarbon generation model of Well MS-1 also showed that the Permian source rock also experienced a hydrocarbon generating and expulsion period, which could provide oil and gas to the Jurassic reservoirs (Fig. 12). The oil source correlation analysis by chromatography provided evidence for this hydrocarbon migration process. The chromatograph of the oil in the Jurassic reservoirs showed a large difference from the chromatograph from the Jurassic source rocks but showed similarity to the chromatograph from the Permian source rock (Fig. 13a, b, c and d). The content of Pr/Ph also showed that the oil in the Jurassic reservoirs showed relative low value of the rate of Pr/Ph, which indicated the semi-deep lake and deep lake environment of source rocks and corresponded to the Permian sources (Fig. 13e). The crude oil carbonate isotope value also showed that the oil from Jurassic reservoirs was characterized by relative low value of carbon isotope which was almost less than -2.8% and similar to the

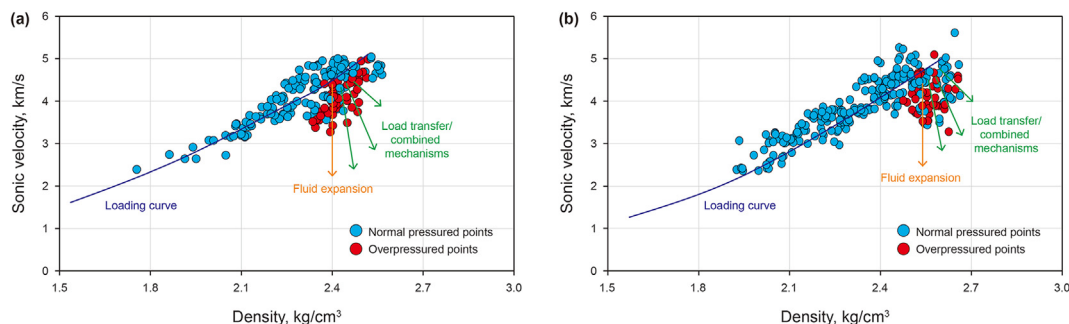


Fig. 10. Overpressure origin analytical results by the sonic velocity-density crossplot method for (a) Well Y-1 and (b) Well Y-2.

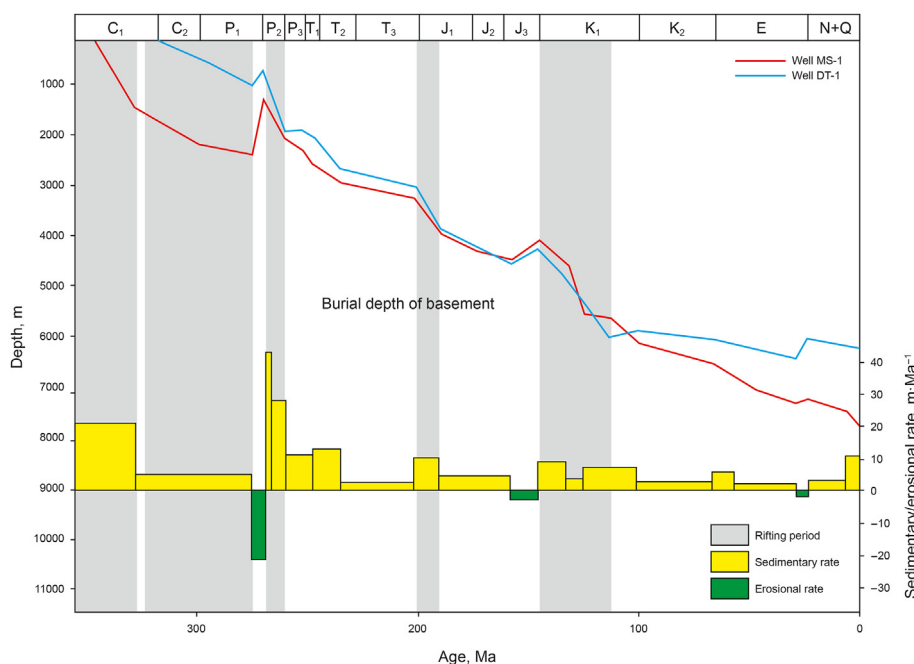


Fig. 11. The general burial history and sedimentary rate of the main geological periods in the CJB. The well locations are shown in Fig. 1.

isotope content in the Permian source rocks (Fig. 13e) (Yang et al., 2011, 2017; Tan et al., 2014). All the analysis indicated that the oil in the Jurassic reservoirs were mainly provided by the Permian source rocks.

Some researchers also stated that although Jurassic source rocks have the potential for hydrocarbon generation, the present oil and gas discovered in the deep-buried Jurassic reservoirs were mainly from the underburden Permian source rocks (Zhao et al., 2015). In addition, the homogenization temperature of the Jurassic deep-buried reservoirs also provided some information about oil and gas charging periods and hence the source of the petroleum in Jurassic reservoirs. The distribution of homogenization temperature was characterized by a unimodal distribution with a peak value of approximately 80–100 °C, which corresponded to the Paleogene period (Fig. 12). The hydrocarbon-generating model showed that in the Late Cretaceous period, the Jurassic source rocks just started to generate hydrocarbons, while the Permian source rocks reached the mature stage and expelled large amounts of hydrocarbons (Fig. 11). Therefore, the oil and gas in the Jurassic reservoirs were mainly from Permian source rocks. In other words, the hydrocarbon generation and migration of the Permian source rocks might have contributed much more to the overpressure in the Jurassic

reservoirs than the hydrocarbon generation of Jurassic source rocks.

5.2.2. Thermal expansion by temperature rise

The variation in temperature is one of the dominant origins of abnormal pressure (Baker, 1972). Many researchers have considered that in deep strata, temperature is the dominant factor for overpressure because of fluid expansion by abnormally high temperatures (Baker, 1972). Owing to the differences in the expansion coefficient, which is defined as the ratio of the increased volume to the original volume when the temperature rises by 1 °C, the formation water, oil, gas and rock skeleton have different volume variations. Previous studies have shown that formation water, oil and gas have larger expansion coefficients than sandstone (Baker, 1972). Therefore, when the temperature rises, the expansion of formation water, oil and gas will be more intensive than the expansion of the rock skeleton and hence lead to overpressure.

As previously stated, the main hydrocarbon injection process lasted from the late middle to the late Cretaceous period. The exploitation data provided by the Shengli oilfield showed that the overpressured reservoirs were dominated by oil production without water and gas production. Note that the formation

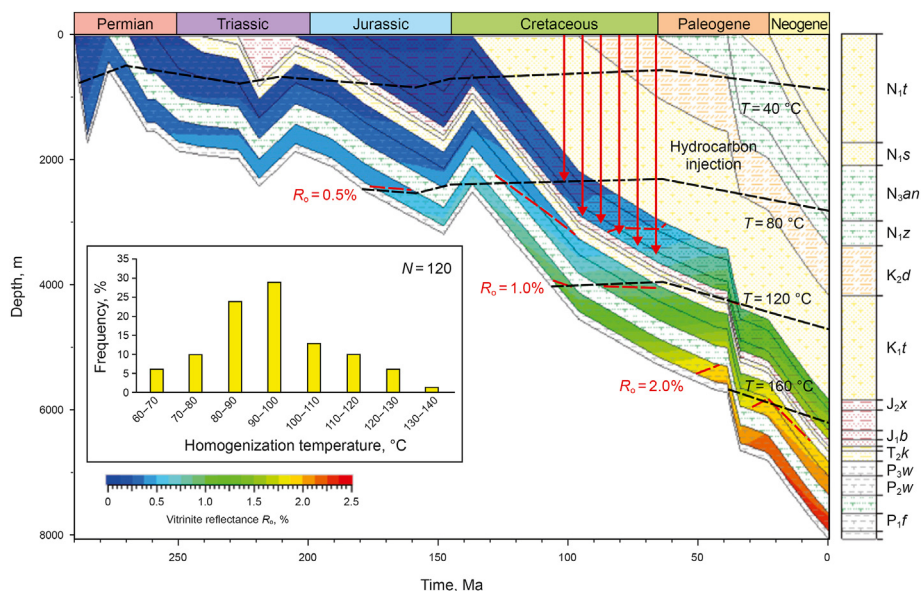


Fig. 12. Hydrocarbon generation and injection of Jurassic and Permian source rocks for Well Y-1 in the CJB.

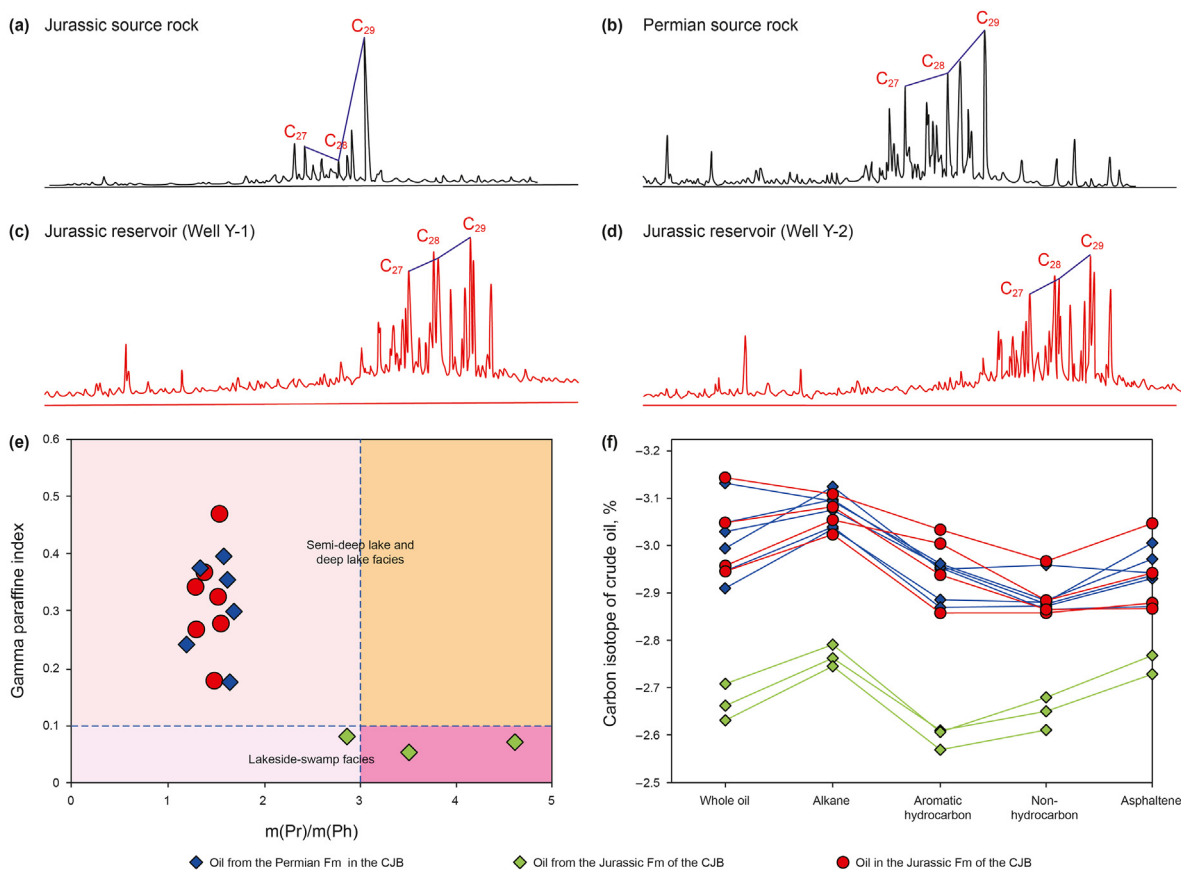


Fig. 13. Comparison of chromatographic data between the oil in Jurassic reservoirs and Jurassic and Permian source rocks in the CJB (Figure (e) and (f) were edited by Yang et al., 2017).

temperature of the bottom of the Jurassic reached 135.9 °C at present (Fig. 14), and the pressure increase by thermal expansion can be roughly calculated by the following equations (Wang et al., 2021):

$$\Delta P_{TE} = \frac{\Delta V}{C_0 \times \varphi} \tag{1}$$

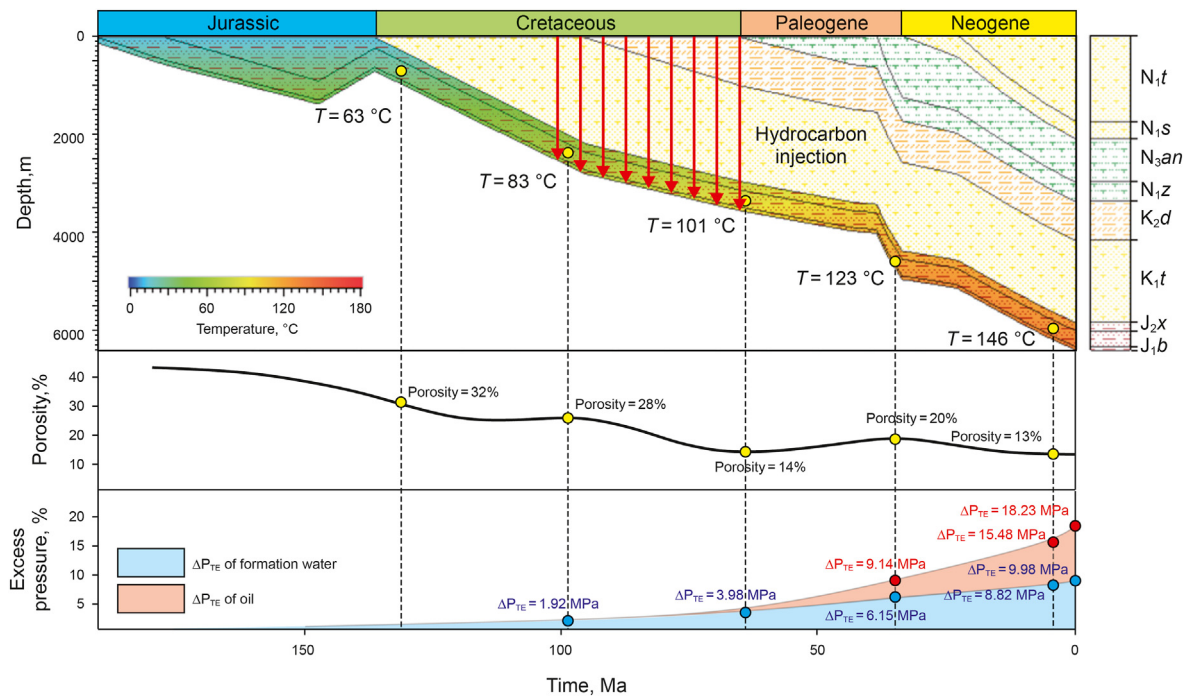


Fig. 14. Thermal and porosity evolution of Well Y-1 in the CJB (Edited by Gao et al., 2017).

$$\Delta V = \Delta T[a_o\phi + a_r(1 - \phi)] \quad (2)$$

where ΔP_{TE} is the pressure increasing by thermal expansion, Pa; ΔV is the expansion of a unit volume, m^3 ; C_o is the oil compressibility, $3 \times 10^{-4} \text{ MPa}^{-1}$ (Russell, 1972); ϕ is the reservoir porosity, dimensionless; ΔT is the temperature increase, K; a_o is the oil expansion coefficient, $9.5 \times 10^{-4} \text{ K}^{-1}$ (Hodgman, 1957); and a_r is the sandstone expansion coefficient, $9 \times 10^{-6} \text{ K}^{-1}$ (Hodgman, 1957).

In this study, the porosity and paleo-porosity data of the Jurassic reservoirs were from published works (Gao et al., 2017). The palaeo-temperature data were from previous studies of thermal history analysis (Qiu et al., 2008; Gao et al., 2017). The calculated results showed that before the main hydrocarbon injection period (middle to late Cretaceous period), the pore fluid was dominated by formation water (whose expansion coefficient was $400 \times 10^{-6} \text{ K}^{-1}$ according to Hodgman, 1957). The excess pressure caused by the rise in temperature increases slowly to approximately 3.96 along with the oil charging and the continuous temperature increase, the pore fluid was dominated by oil (expansion coefficient was $950 \times 10^{-6} \text{ K}^{-1}$ according to Hodgman, 1957). The excess pressure increased quickly. Finally, the volume expansion of oil could lead to 18.23 MPa excess pressure at present in the deep-buried sandstone reservoirs in the CJB, which indicates that thermal expansion has a significant contribution to the overpressure in the CJB. In addition, we also calculated the pressure variation without oil charging. The results showed that when the reservoir was full of formation water, the fluid expansion could cause approximately 9.98 MPa excess pressure, which was much lower than the excess pressure caused by the oil layer. Therefore, the intensive overpressure in the deep strata might be a signal for hydrocarbon accumulation.

5.3. Tectonic compression and pressure transfer by faults

5.3.1. Tectonic compression of the Junggar Basin

Tectonic compression is also considered one of the important

sources of overpressure, especially in some basins or regions that experienced multistage tectonic movements (Berry, 1973). Previous studies indicated that the Junggar Basin experienced tectonic compression in both the east–west and north–south directions (He et al., 2018). In the north–south trend, the tectonic evolutionary reconstruction results showed that the length of profile B–B' (the location is shown in Fig. 1) has been shortened by approximately 43 km with a shortening rate of 12.2%. The tectonic compression first led to shortening of the B–B' profile by 11 km during the middle to late Permian period and the end of the Paleogene, then led to intensive compression with shortening of the profile by 30 km. Although there were some extension processes, the CJB was characterized by compressive features trending north–south (Fig. 15).

The intensity of compression in the east–west direction was stronger than that in the north–south direction (Fig. 16). The length of profile C–C' (the location is shown in Fig. 1) has been shortened by approximately 302 km with a shortening rate of 35.8% owing to five main compression processes. The first compression lasted from the middle to late Permian with the shortening of the B–B' profile by 112 km. The second compression during the Early Triassic caused the shortening by 90 km. The third compression during the Middle to Late Triassic led to the shortening of the profile by 11 km. The fourth compression during the Early to Middle Jurassic led to the shortening of the profile by 52 km. The fifth compression during the Middle to Late Jurassic caused the shortening of the profile by 15 km (Fig. 15).

To conclude, the whole Junggar Basin experienced intensive tectonic compression, and the east–west-trending compression was more intensive than the north–south-trending compression. Considering that the overpressure we analysed was mainly in Jurassic reservoirs, the periods of tectonic compression should be noted. The compression before and after the Jurassic period may have different contributions to the overpressure in the Jurassic sediments. First, the compression after the Jurassic periods can compress the sand bodies of Jurassic Formations directly and hence

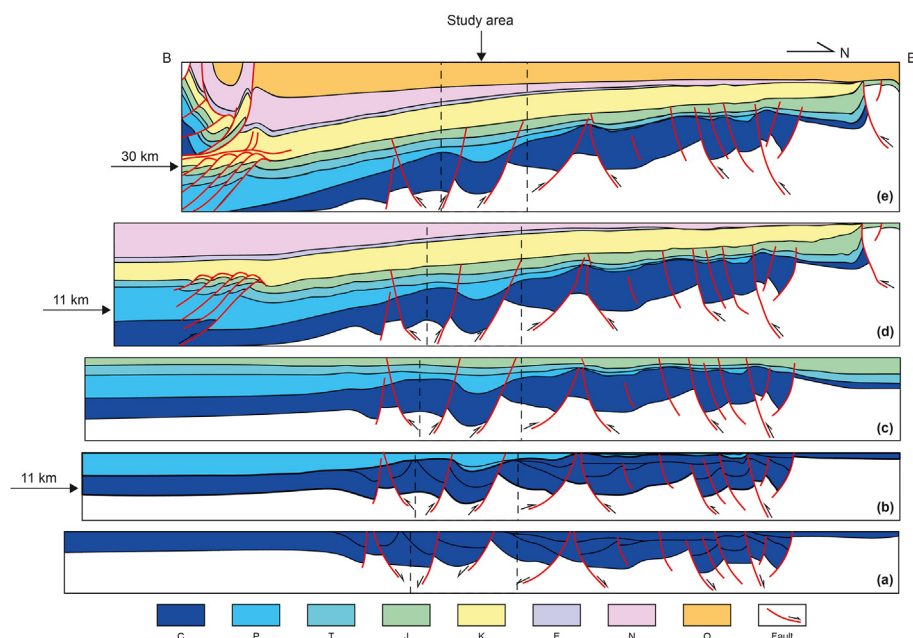


Fig. 15. North-south trending tectonic evolution profile (B–B') of the Junggar Basin. The location of the profile is shown in Fig. 1.

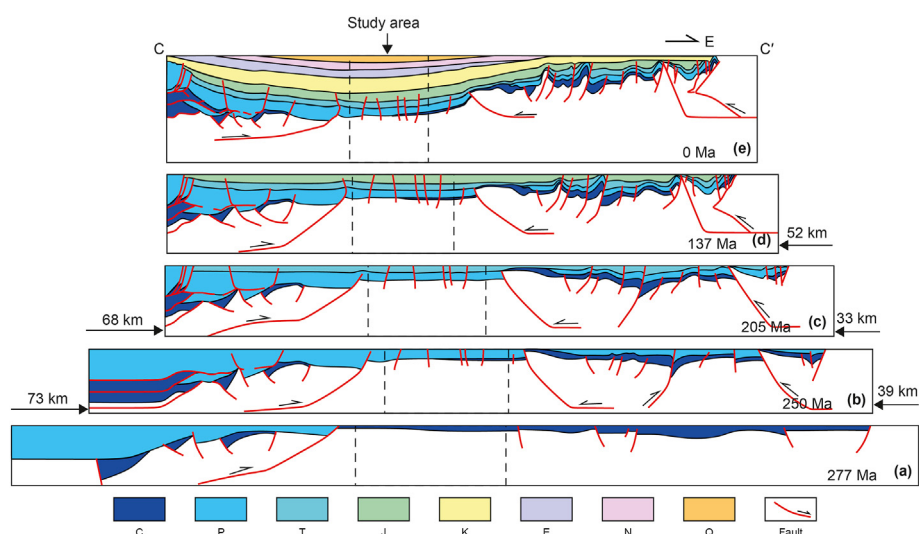


Fig. 16. North-south trending tectonic evolution profile (C–C') of the Junggar Basin. The location of the profile is shown in Fig. 1.

lead to overpressure. Comparing the tectonic compression processes in different trends, it is found that the compression after Jurassic periods developed in both W-E-trending and N-S-trending directions, which indicated that direct compression was developed and hence contributed to the overpressure in the Jurassic reservoirs (Figs. 15 and 16).

5.3.2. Pressure transfer by developed faults

In addition to the direct compression of the sand bodies after the Jurassic period, the more intensive compression in the W-E trend occurred before the Jurassic periods. Such intensive compression could have led to massive overpressure accumulation in Carboniferous, Permian and Triassic sediments. Considering that the Permian mudstones were the main source rocks in the CJB, the overpressure in the Permian strata could be more developed. Furthermore, along with tectonic compression, different sizes of

faults developed during the Permian to Jurassic periods.

Over 50 faults have been discovered in the study area, which are dominated by reverse faults and strike-slip faults with large fault dip angles. Some of the faults were characterized by large scales and developed from the Permian to the Cretaceous formations (Fig. 17). The geometric features of the faults were different from deep to shallow. The faults in the Permian formation were characterized by reticular structures with many branches from depths of 9000–11,000 m. This geometric feature indicated that the compression in the Permian formation was more intensive. In addition, the overpressured geofluids (hydrocarbon) generated in the source rocks in the Permian formation could more easily migrate to shallower depths along the developed branches of faults. The middle part of the faults in the Triassic formation was characterized by flower-like structures. The branches of the faults in this part were less than those in the Permian formation, which showed

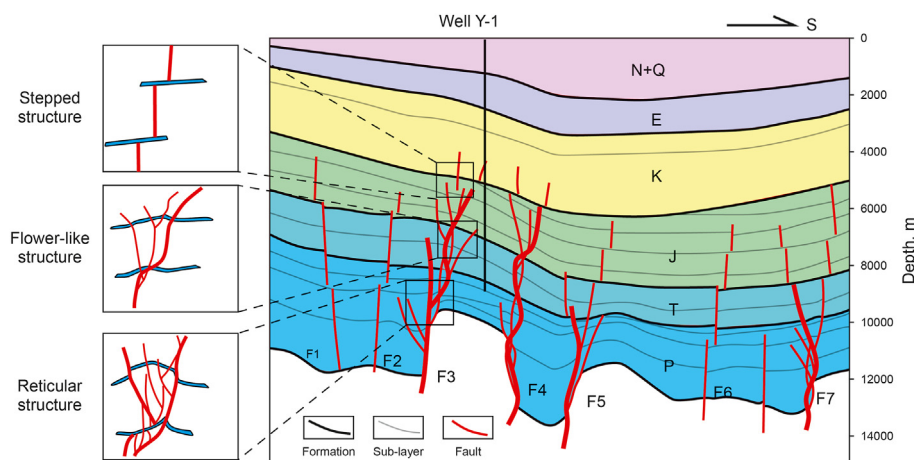


Fig. 17. Geometric characteristics of the CJB faults. The figure shows the main faults with typical fault structures in the CJB instead of all the faults.

that the compression in the Triassic formation was lower than that in the Permian formation. These branches could also provide high-efficiency pathways for the migration of overpressured geofluids with oil and gas. The faults in the Jurassic formation were dominated by a stepped structure, which was characterized by a single branch. This structure of the faults indicated that the migrating capability of the faults in the Jurassic formation was relatively weaker than that in the Triassic and Permian formations, but these faults were also effective in hydrocarbon migration, especially when the overpressure in the underburden strata can provide enough driving forces. Note that most of the faults were terminated in Jurassic formations, which showed that the sandstones in Jurassic were the destination of the vertical migration of hydrocarbons and hence the dominant oil and gas accumulation reservoirs in the study area. Therefore, the overpressure generated in the deep strata by hydrocarbon generation could be transferred to the Jurassic sandstone reservoirs by faults.

In addition to the distribution of the faults, the evolution of the faults and hydrocarbon generation were also important for pressure transfer. In this study, the activity of the main faults in the CJB was characterized by the fault activity rate (abbreviated as FAR), which can be calculated using the following equation:

$$\text{Fault activity rate} = \frac{\text{Paleo fall}}{\text{Time of fault activity}} \quad (3)$$

Based on the seismic interpretation and the tectonic movement history analysis, we calculated the FAR for 7 main developed faults, as shown in Fig. 16. The results showed similar evolutionary processes of fault activity for the 7 faults. During Permian periods, the FAR was always less than 2 m/Ma, which showed the inactive feature of faults. During the Triassic period, all the faults were active with the rapidly increasing FAR. The FAR in this period increased to 2–10 m/Ma. The fault activity decreased in the Jurassic period but remained in a relatively active state, with the FAR decreasing to approximately 0.7–4.2 m/Ma. In the Cretaceous period, all the faults remained almost steady without activity (Fig. 18). As previously stated, the main hydrocarbon injection period was the Late Cretaceous period, during which the main faults had already formed and developed. Therefore, overpressured geofluids with hydrocarbons in Permian source rocks can vertically migrate to Jurassic sandstone reservoirs along faults.

6. Pore pressure evolution and hydrocarbon accumulation model

The overpressure sources and pore pressure evolutionary processes are closely related to the hydrocarbon accumulation processes, which are reflected in hydrocarbon generation and migration. In this study, the aim of the pressure evolution model was to show the overpressure origins under the background of petroleum geology. A number of qualitative and quantitative processes were used in the construction of the pressure evolution model, including the tectonic movements, thermal history, hydrocarbon generating history and migrating processes. The evolution of pore pressure evolution along with the hydrocarbon generation could be divided into three stages.

- (1) Early-period tectonic compression stage (Carboniferous to Jurassic periods from 350 to 250 Ma): During this period, the Jurassic strata were deposited, and the source rocks in Permian and Jurassic Formations were at an immature stage without hydrocarbon generation. The sandstone reservoirs in the Jurassic Formation were filled by formation water. Continuous tectonic compression during this stage led to the development of faults (Fig. 19a). Therefore, the overpressure mainly developed in the Carboniferous, Permian and Triassic strata by intensive tectonic compression (Fig. 19b).
- (2) Hydrocarbon generating and migrating stage (Jurassic to Cretaceous periods from 250 to 137 Ma): With the deep burial of strata, hydrocarbon generation occurred in the source rocks of the Permian strata and led to overpressure in the source rocks. Meanwhile, the tectonic compression in this period aggravated the overpressure and generated more faults of different sizes, which provided migrating pathways for hydrocarbon migration and overpressure transfer in the vertical direction. When the overpressure in the source rocks was large enough, hydrocarbons migrated from the source rocks in the Permian strata to the Jurassic strata in the vertical direction through faults and microfractures. The excess pressure in the Jurassic sandstone reservoirs gradually increased with the hydrocarbon migration process. Note that during this period, the source rocks in the Jurassic Formation were still in an immature stage without hydrocarbon generation (Fig. 19c). Therefore, during this period, the overpressure in the Jurassic mudstone was mainly from tectonic

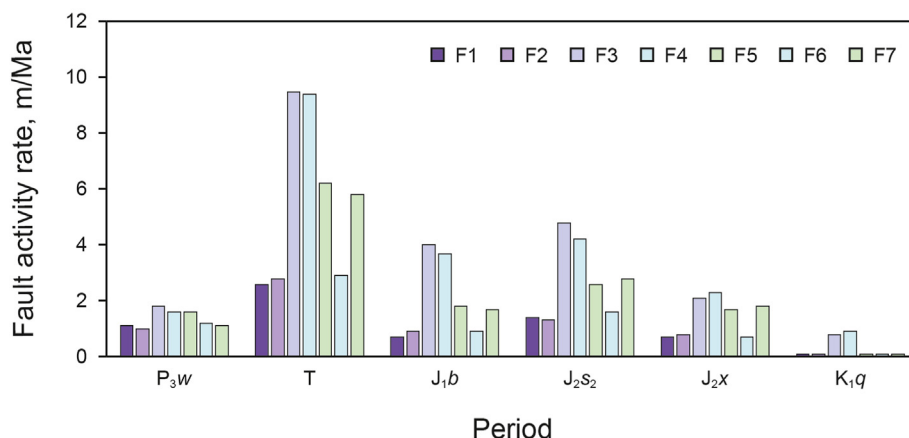


Fig. 18. The evolution of the fault activity rate for 7 main developed faults in the CJB. The locations of the faults are marked in Fig. 16.

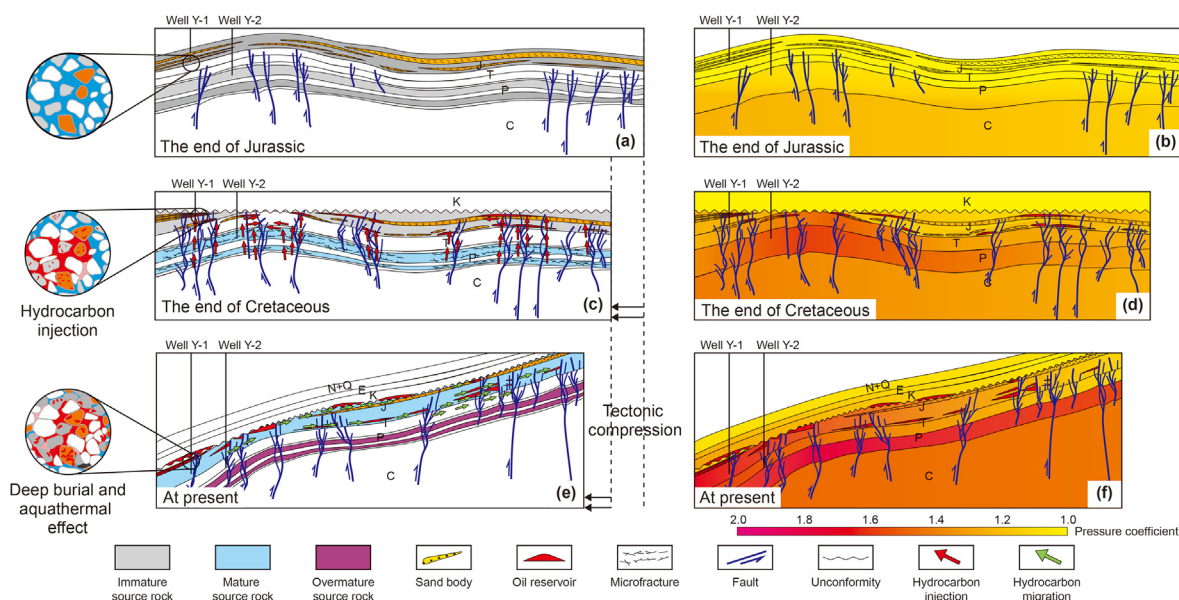


Fig. 19. Pressure evolution and hydrocarbon accumulation model.

compression, while the overpressure in the Jurassic sandstone reservoirs was mainly from pressure transfer by hydrocarbon migration from Permian sources (Fig. 19d). These processes indicated that overpressure was a significant driving force of hydrocarbon migration. The hydrocarbons would more easily migrate with the overpressure developed.

(3) Deep burial and aquathermal stage (Palaeogene periods to the present from 100 to 0 Ma): From this period, the burial depth of the overpressured strata increased from approximately 4000 m–6000 m, which led to pressure increases by the aquathermal effect. Furthermore, continuous tectonic compression in the south-north trend also enhanced the overpressure in the Jurassic strata, which was the main hydrocarbon accumulating reservoir in the CJB. In addition, hydrocarbon generation occurred and led to pressure increases in the Jurassic source rocks (Fig. 19e). Therefore, the overpressure in Jurassic mudstone increased by continuous tectonic compression, hydrocarbon generating processes and aquathermal effects. The overpressure in Jurassic sandstone

reservoirs also increases, which is dominated by the aquathermal effect. Continuous tectonic compression also contributes to the increase in overpressure (Fig. 19f). Owing to the disparity of the aquathermal effect between oil (gas) and formation water, the development of intensive overpressure may indicate the accumulation of oil and gas, especially for deeply buried reservoirs.

7. Conclusions

- (1) The deep-buried strata in the central portion of the Junggar Basin were characterized by intensive overpressure, especially in Jurassic strata. The Pcoe of the overpressured Jurassic strata mainly ranged from 1.4 to 1.8 and even reached approximately 1.93 from depths of approximately 4800 m–6200 m.
- (2) The sources of the overpressure in the CJB are complex. The results from Bowers' and sonic velocity-density method

showed that the overpressure was caused by multiple possible sources including fluid expansion, tectonic compression and pressure transfer.

- (3) The geological processes provided more evidence for generating and evolutionary processes of the overpressure. The hydrocarbon generation in the Jurassic source rocks led to pressure increases in the mudstones, while the oil source correlation analysis showed that the overpressure in the Jurassic sandstone reservoirs was due to pressure transfer in the vertical direction from the overpressured fluids generated in the Permian source rocks. Increases in temperature along deep burial induced pressure increases through thermal expansion of pore fluids, and the continuous tectonic compression from the Carboniferous period to the present also contributed to overpressure in the CJB.
- (4) The evolution and distribution of overpressure could provide evidence and guidance for hydrocarbon migration and accumulation. As a significant driving force of hydrocarbons, overpressure indicated possible vertical migration pathways of hydrocarbons. In addition, owing to the disparity in the acoustic effect between oil (gas) and formation water, the intensive overpressure indicated the accumulation of hydrocarbons in deeply buried reservoirs.

Declaration of competing interest

No conflict of interest exists in the submission of this manuscript, and manuscript is approved by all authors for publication. I would like to declare on behalf of my co-authors that the work described was original research that has not been published previously, and not under consideration for publication elsewhere, in whole or in part. All the authors listed have approved the manuscript that is enclosed.

Acknowledgements

This study was supported by the National Natural Science Foundation of China (Grant No. 41972124). We gratefully acknowledge the Shengli Oilfield Branch of the China Petroleum & Chemical Corporation for providing field test data and reservoir data.

References

Abdel-Fattah, M.I., Pigott, J.D., Abd-Allah, Z.M., 2017. Integrative 1D-2D basin modelling of the cretaceous beni suief basin, western desert, Egypt. *J. Pet. Sci. Eng.* 153, 297–313. <https://doi.org/10.1016/j.petrol.2017.04.003>.

Baker, C., 1972. Aquathermal pressuring-role of temperature in the development of abnormal pressure zones. *AAPG Bull.* 56 (10), 2068–2871. <https://doi.org/10.1306/819A41B0-16C5-11D7-8645000102C1865D>.

Berry, F., 1973. High fluid potentials in California Coast ranges and their tectonic significance. *AAPG Bull.* 57 (7), 1219–1249. <https://doi.org/10.1306/83D90E8A-16C7-11D7-8645000102C1865D>.

Birchall, T., Senger, K., Hornum, M.T., et al., 2021. Underpressure in the northern Barents shelf: causes and implications for hydrocarbon exploration. *AAPG Bull.* 104 (11), 2267–2295. <https://doi.org/10.1306/02272019146>.

Bowers, G.L., 2002. Detecting high overpressure. *Lead. Edge* 21 (2), 174–177. <https://doi.org/10.1190/1.1452608>.

Caillet, G., Judge, N.C., Bramwell, N.P., et al., 1997. Overpressure and hydrocarbon trapping in the chalk of the Norwegian central graben. *Petrol. Geosci.* 3 (1), 33–42. <https://doi.org/10.1144/petgeo.3.1.33>.

Cao, J., Wang, X.L., Sun, P.A., et al., 2012. Geochemistry and origins of natural gases in the central Junggar Basin, northwest China. *Org. Geochem.* 53, 166–176. <https://doi.org/10.1016/j.orggeochem.2012.06.009>.

Cao, J., Yao, S.P., Jin, Z.J., et al., 2006. Petroleum migration and mixing in the northwestern Junggar Basin (NW China): constraints from oil-bearing fluid inclusion analyses. *Org. Geochem.* 37 (7), 827–846. <https://doi.org/10.1016/j.orggeochem.2006.02.003>.

Dai, J.X., Zou, C.N., Li, J., et al., 2009. Carbon isotopes of Middle–Lower Jurassic coal-derived alkane gases from the major basins of northwestern China. *Int. J. Coal Geol.* 80 (2), 124–134. <https://doi.org/10.1016/j.coal.2009.08.007>.

Fan, Z.Q., Jin, Z.H., Johnson, S.E., 2012. Modelling petroleum migration through microcrack propagation in transversely isotropic source rocks. *Geophys. J. Int.* 190 (1), 179–187. <https://doi.org/10.1111/j.1365-246X.2012.05516.x>.

Gao, C.L., Ji, Y.L., Gao, Z.Y., et al., 2017. Multi-factor coupling analysis on property preservation process of deep buried favourable reservoir in Hinterland of Junggar Basin. *Acta Sedimentol. Sin.* 35 (3), 577–591. <https://doi.org/10.14027/j.cnki.cjxb.2017.03.015>.

Guo, X.W., He, S., Liu, K.Y., et al., 2019. Generation and evolution of overpressure caused by hydrocarbon generation in the Jurassic source rocks of the central Junggar Basin, northwestern China. *AAPG Bull.* 103 (7), 1553–1574. <https://doi.org/10.1306/1213181614017139>.

Hakimi, H.M., Alaug, A.S., Mohialdeen, J., et al., 2019. Late Jurassic Arwa Member in south-eastern Al-Jawf sub-basin, NW Sabatayn Basin of Yemen: geochemistry and basin modelling reveal shale-gas potential. *J. Nat. Gas Sci. Eng.* 64, 133–151. <https://doi.org/10.1016/j.jngse.2019.01.022>.

Hao, F., Zhang, Z.H., Zou, H.Y., et al., 2011. Origin and mechanism of the formation of the low-oil saturation Moxizhuang field, Junggar Basin, China: implication for petroleum exploration in basins having complex histories. *AAPG Bull.* 95 (6), 983–1008. <https://doi.org/10.1306/11191010114>.

He, D.F., Zhang, L., Wu, S.T., et al., 2018. Tectonic evolution stages and features of the Junggar Basin. *Oil Gas Geol.* 39 (5), 845–861. <https://doi.org/10.11743/ogg20180501> (in Chinese).

He, S., He, Z.L., Yang, Z., 2009. Characteristics, well-log responses and mechanisms of overpressure within the Jurassic formation in the central part of Junggar Basin. *J. Earth Sci.* 34 (3), 457–470. [doi.org/10.1002/2383\(2009\)03<0457::JG>3.0.CO;2](https://doi.org/10.1002/2383(2009)03<0457::JG>3.0.CO;2) (in Chinese).

He, W.J., Fei, L.Y., Ablimiti, Y.M., et al., 2019. Accumulation conditions of deep hydrocarbon and exploration potential analysis in Junggar Basin, NW China. *Earth Sci. Front.* 26 (1), 189–201. <https://doi.org/10.13745/j.esf.sf.2019.1.12>.

Hodgman, C.D., 1957. *Handbook of Chemistry and Physics*. Chemical Rubber Pub Press, Ohio, pp. 3213–3214.

Hunt, J.M., 1990. Generation and migration of petroleum from abnormally pressured fluid compartments. *AAPG Bull.* 74 (1), 1–12. <https://doi.org/10.1029/JB095iB01p00649>.

Jin, Z.H., Johnson, S.E., 2008. Primary oil migration through buoyancy-driven multiple fracture propagation: oil velocity and flux. *Geophys. Res. Lett.* 35 (9), 250–258. <https://doi.org/10.1029/2008GL033645>.

Lahann, R.W., Swarbrick, R.E., 2011. Overpressure generation by load transfer following shale framework weakening due to smectite diagenesis. *Geofluids* 11 (4), 362–375. <https://doi.org/10.1111/j.1468-8123.2011.00350.x>.

Lash, G.G., Engelder, T., 2005. An analysis of horizontal microcracking during catagenesis: example from the Catskill delta complex. *AAPG Bull.* 89 (11), 1433–1449. <https://doi.org/10.1306/05250504141>.

Law, B.E., Dickinson, W.W., 1985. Conceptual-model for origin of abnormally pressured gas accumulation in low-permeability reservoirs. *AAPG Bull.* 69 (8), 1295–1304. <https://doi.org/10.1306/AD462BD7-16F7-11D7-8645000102C1865D>.

Law, B.E., Spencer, C.W., 1998. Abnormal pressure in hydrocarbon environments. *AAPG Mem* 70, 1–11. <https://doi.org/10.0000/PMID14065>.

Li, J., Zhao, J.Z., Hou, Z.Q., et al., 2021. Origins of overpressure in the central Xihu depression of the East China Sea shelf basin. *AAPG Bull.* 105 (8), 1627–1659. <https://doi.org/10.1306/02262118112>.

Liu, J.D., Liu, T., Liu, H., et al., 2021a. Overpressure caused by hydrocarbon generation in the organic-rich shales of the Ordos Basin. *Mar. Petrol. Geol.* 134, 105349. <https://doi.org/10.1016/j.marpetgeo.2021.105349>.

Liu, J.D., Zhang, C.J., Jiang, Y.L., et al., 2021b. Paleo-pressure evolution of reservoir and its main controlling factors in the third member of xujiahe formation in Yuanba area, sichuan basin. *J. China Univ. Pet., Ed. Nat. Sci* 45 (2), 31–41. <https://doi.org/10.3969/j.issn.1673-5005.2021.02.004> (in Chinese).

Liu, Y.F., Qiu, N.S., Xie, Z.Y., et al., 2016. Overpressure compartments in the central paleo-uplift, sichuan basin, southwest China. *AAPG Bull.* 100 (5), 867–888. <https://doi.org/10.1306/02101614037>.

Osborne, M.J., Swarbrick, R.E., 1997. Mechanisms for generating overpressure in sedimentary basins: a reevaluation. *AAPG Bull.* 81 (6), 1023–1041. <https://doi.org/10.1093/jietcom/e90-b.2.425>.

Qiu, N., Zhang, Z., Xu, E., 2008. Geothermal regime and Jurassic source rock maturity of the Junggar Basin, northwest China. *J. Asian Earth Sci.* 31 (4), 464–478. <https://doi.org/10.1016/j.jseas.2007.08.001>.

Roberts, S.J., Nunn, J.A., 1995. Episodic fluid expulsion from geopressed sediments. *Mar. Petrol. Geol.* 12 (2), 195–204. [https://doi.org/10.1016/0264-8172\(95\)92389-0](https://doi.org/10.1016/0264-8172(95)92389-0).

Russell, W.L., 1972. Pressure-depth relations in Appalachian region. *AAPG Bull.* 56 (3), 528–536. [https://doi.org/10.1016/0041-1647\(71\)90038-4](https://doi.org/10.1016/0041-1647(71)90038-4).

Schofield, N., Holford, S., Edwards, A., et al., 2019. Overpressure transmission through interconnected igneous intrusions. *AAPG Bull.* 104 (2), 285–303. <https://doi.org/10.1306/05091918193>.

Swarbrick, R.E., Osborne, M.J., 1998. Mechanisms that generate abnormal pressures: an overview. *AAPG Mem* 70, 13–34. <https://doi.org/10.1306/M70615C2>.

Tan, S., Zeng, Z.P., Gong, Y.J., et al., 2014. Control of abnormal overpressure on hydrocarbon-reservoir evolution and hydrocarbon filling process in central of Junggar Basin. *Fault-Block Oil Gas Field* 21 (3), 287–291. <https://doi.org/10.6056/dkyqt201403004> (in Chinese).

Teige, G., Hermannrud, C., Wensaas, L., et al., 1999. The lack of relationship between overpressure and porosity in North Sea and Haltenbanken shales. *Mar. Petrol. Geol.* 16 (4), 321–335. [https://doi.org/10.1016/S0264-8172\(98\)00035-X](https://doi.org/10.1016/S0264-8172(98)00035-X).

- Timko, D.J., Fertl, W.H., 1971. Relationship between hydrocarbon accumulation and geopressure and its economic significance. *J. Petrol. Technol.* 23 (8), 923–933. <https://doi.org/10.2118/2990-PA>.
- Tingay, P., Hillis, R., Swarbrick, R.E., et al., 2007. Vertically transferred” overpressures in Brunei: evidence for a new mechanism for the formation of high magnitude overpressures. *Geology* 35 (11), 1023–1026. <https://doi.org/10.1130/G23906A.1>.
- Tingay, P., Hillis, R., Swarbrick, R.E., et al., 2009. Origin of overpressure and pore pressure prediction in the Baram Delta Province, Brunei. *AAPG Bull.* 93 (1), 51–74. <https://doi.org/10.1306/08080808016>.
- Tingay, P., Morley, C.K., Laird, A., et al., 2013. Evidence for overpressure generation by kerogen-to-gas maturation in the northern Malay Basin. *AAPG Bull.* 97 (4), 639–672. <https://doi.org/10.1306/09041212032>.
- Ungerer, P., Burrus, J., Doligez, B., et al., 1990. Basin evaluation by integrated two-dimensional modelling of heat transfer, fluid flow, hydrocarbon generation, and migration. *AAPG Bull.* 74 (3), 309–335. <https://doi.org/10.1306/0C9B22DB-1710-11D7-8645000102C1865D>.
- Wang, Q.C., Chen, D.X., Gao, X.Z., et al., 2021. Evolution of abnormal pressure in the Paleogene E3 formation of the huimin depression, bohai bay basin, China. *J. Pet. Sci. Eng.* 203, 108601. <https://doi.org/10.1016/j.petrol.2021.108601>.
- Webster, M., O'Connor, S., Pindar, B., et al., 2011. Overpressures in the Taranaki basin: distribution, causes, and implications for exploration. *AAPG Bull.* 95 (3), 339–370. <https://doi.org/10.1306/06301009149>.
- Xiao, Q., He, S., Yang, Z., et al., 2010. Petroleum secondary migration and accumulation in the central Junggar Basin, northwest China: insights from basin modeling. *AAPG Bull.* 94 (7), 937–955. <https://doi.org/10.1306/12090909002>.
- Yang, Z., He, S., He, Z.L., 2008. Distribution of overpressure stratum and its relationship with hydrocarbon accumulation in the central part of Junggar basin. *Acta Pet. Sin.* 29 (2), 199–205. <https://doi.org/10.1111/j.1365-2427.2008.01957.x> (in Chinese).
- Yang, Z., He, S., Li, Q.Y., et al., 2016. Geochemistry characteristics and significance of two petroleum systems near top overpressured surface in central Junggar Basin, NW China. *Mar. Petrol. Geol.* 75, 341–355. <https://doi.org/10.1016/j.marpetgeo.2016.04.025>.
- Yang, Z., He, S., Zhang, Y.G., et al., 2017. Oil geochemical characteristics near the top overpressured surface in central Junggar Basin. *J. Shenzhen Univ., Sci. Eng.* 34 (4), 331–343. <https://doi.org/10.3724/SP.J.1249.2017.04331> (in Chinese).
- Yang, Z., Wang, J.H., Lin, S.H., 2011. Hydrocarbon accumulation mechanism near top of overpressured surface in central Junggar Basin. *J. China Univ. Pet., Ed. Nat. Sci* 35 (3), 19–25. <https://doi.org/10.1007/s12182-011-0123-3> (in Chinese).
- Zhang, H., Pang, X.Q., Jiang, Z.X., 2005. A study of the overpressures of the Kela-2 gas field in the Kuqa depression. *Acta Geosci. Sin.* 26 (2), 163–168. <https://doi.org/10.3321/j.issn:1006-3021.2005.02.010> (in Chinese).
- Zhao, H., Luo, X.R., Zhang, L.K., et al., 2015. A sign to the multi-phases hydrocarbon charge and adjustment: fluid inclusion study from the Sangonghe Formation in the No.1 block, the middle Junggar Basin. *Nat. Gas Geosci.* 26 (3), 466–476. <https://doi.org/10.11764/j.issn.1672-1926.2014.03.0466> (in Chinese).
- Zhao, J., 2003. *Theory of Gas Pool-Forming in Foreland Basin and its Application*. Petroleum Industry Press, Beijing, pp. 190–191 (in Chinese).
- Zhao, J.Z., Li, J., Xu, Z., 2017. Advances in the origin of overpressures in sedimentary basins. *Acta Pet. Sin.* 38 (9), 973–998. <https://doi.org/10.7623/syxb201709001> (in Chinese).